Tellus (1984), *36A*, 30–41

On the existence of solutions to Machenhauer's non-linear normal mode initialization

By LENNART THANING*, *Department of Meteorology*[1], *University of Stockholm, Arrhenius Laboratory, S-10691 Stockholm, Sweden*

(Manuscript received December 17, 1982; in final form May 2, 1983)

ABSTRACT

The existence of solutions to the non-linear normal mode initialization proposed by Machenhauer is examined in a low-order version of a shallow water model on an equatorial β-plane. The model contains only three modes: one Rossby mode and two gravity type modes. Simple physical forcing is included in the model.

The analysis shows that generally there is more than one state that satisfies the initial conditions. Only one, however, can be accepted as a realistic initial state. Furthermore, in the case without non-adiabatic forcing, the iterative non-linear normal mode procedure can converge only to the realistic initial state. When the Rossby amplitude is increased beyond a critical value, the realistic initial state ceases to exist. The critical value of the Rossby amplitude decreases when the fluid becomes more shallow. Non-adiabatic forcing may also violate the existence of the realistic initial state. The critical forcing necessary to do this, decreases with decreasing depth of the fluid.

1. Introduction

Models used for weather forecasting based on the primitive equations have been used since the early 1960s. These models are, unlike the filtered models used earlier, able to describe high-frequency oscillations (gravity waves). If the initial state is not properly chosen, the gravity waves tend to get unrealistically large amplitudes. Through the years, there have been several approaches on how to balance the wind field against the height field initially, in order to avoid unrealistically large high-frequency oscillations. The most successful ones have been the so-called non-linear normal mode initializations proposed by Machenhauer (1977) and Baer (1977). In these methods the physical variables are projected on the normal modes of the linearized equations. In principle, the normal modes are divided into two different classes: the low-frequency Rossby modes and the high-frequency gravity modes. Machenhauer requires the initial tendencies of the gravity modes to be zero while Baer assumes the amplitudes of the normal modes to be dependent of two time scales, one fast and one slow, and requires that the variations on the fast time scale disappear.

The Machenhauer procedure has been incorporated in the ECMWF (European Centre for Medium Range Weather Forecasts) forecasting model and in that context has proved to be very effective in removing spurious oscillations from the forecast. However, some problems have also appeared. Temperton and Williamson (1979) reported that the procedure diverges for small values of the equivalent depth. They also found that when forcing due to diabatic effects was included in the procedure, the divergence occurred for even larger values of the equivalent depth. Tribbia (1981) showed that in a low-order model on an f-plane, there is no solution to the height-constrained Machenhauer initialization for certain height fields, indicating that the problem with

[1] Contribution No. 485.

* Present affiliation: National Defense Research Institute, S-90182 Umeå, Sweden.

divergence might be a fundamental and not a numerical problem.

This work is an attempt to gain some insight into the problems concerning the divergence of the unconstrained Machenhauer initialization procedure by using a low-order shallow water model on an equatorial β-plane. The model, which is written in normal mode form (Gollvik and Thaning, 1980), contains only three modes: one Rossby mode and two gravity-type modes. The small number of variables in the model enables us to partly use analytical methods.

The model is discussed in Section 2. Section 3 contains the analysis in the no-forcing case while the effects of simple diabatic forcing are considered in Section 4. A summary is given in Section 5.

2. The model

The model used in this investigation is a low-order version of a shallow water model on an equatorial β-plane, written in normal-mode form, described by Gollvik and Thaning (1980). A very similar model was used by Tribbia (1979). The governing equations are:

$$\frac{\partial u}{\partial t} - \theta v + \frac{\partial \phi}{\partial \lambda} = -\varepsilon\left[u\frac{\partial u}{\partial \lambda} + v\frac{\partial u}{\partial \theta}\right], \tag{2.1}$$

$$\frac{\partial v}{\partial t} + \theta u + \frac{\partial \phi}{\partial \theta} = -\varepsilon\left[u\frac{\partial v}{\partial \lambda} + v\frac{\partial v}{\partial \theta}\right], \tag{2.2}$$

$$\frac{\partial \phi}{\partial t} + \kappa^{-1}\left(\frac{\partial u}{\partial \lambda} + \frac{\partial v}{\partial \theta}\right) = -\varepsilon\left[\frac{\partial u\phi}{\partial \lambda} + \frac{\partial v\phi}{\partial \theta}\right], \tag{2.3}$$

where u, v and ϕ are perturbations from the state of rest and from the mean geopotential $\Phi = gH$, respectively. Furthermore (u,v,ϕ,t) are scaled with $(U,U,2\Omega r_a\, U,1/2\Omega)$ and $\lambda = x/r_a$; $\theta = u/r_a$ (r_a is the radius and Ω is the rotational frequency of the earth).

$$\kappa = \frac{4\Omega^2 r_a^2}{\Phi} \quad \text{and} \quad \varepsilon = \frac{U}{2\Omega r_a}$$

are two non-dimensional numbers, corresponding to the Lamb parameter and the planetary Rossby number, respectively. If we rewrite eqs. (2.1)–(2.3) in normal mode form we get a system of ordinary differential equations:

$$\frac{\mathrm{d}}{\mathrm{d}t} D_{m,n,j} + i\sigma_{m,n,j} D_{m,n,j} = -\varepsilon \times \left(\sum_{k=-M}^{M}\sum_{l=n'}^{N}\sum_{l'=n'}^{N}\sum_{i=1}^{3}\sum_{i'=1}^{3} D_{m-k,l',i'} D_{k,l,i} \times W^{m,n,j}_{k,l,l',i,i'}\right) \tag{2.4}$$

Here the W's are the interaction coefficients and $D_{m,n,j}$ is the complex amplitude of an eigensolution $\hat{\Upsilon}_{m,n,j}$ to the linear part of system (2.1)–(2.3):

$$\begin{pmatrix}\hat{u}\\ \hat{c}\\ \hat{\phi}\end{pmatrix} = \begin{pmatrix} \kappa^{1/4}(A_{m,n,j}H_{n-1}(\eta) - B_{m,n,j}H_{n+1}(\eta)) \\ C_{m,n,j}H_n(\eta) \\ \kappa^{-1/4}(-A_{m,n,j}H_{n-1}(\eta) - B_{m,n,j}H_{n+1}(\eta)) \end{pmatrix} e^{-\eta^2/2 + im\lambda} \tag{2.5}$$

where

$\eta = \kappa^{1/4}\theta$

H_n = a Hermite polynomial of order n (when n is even (odd) H_n is symmetric (antisymmetric) with respect to the equator)

m = the zonal wavenumber

n = a meridional index

j = mode index ($j = 1$ refers to a Rossby mode, $j = 2, 3$ refer to gravity-inertia modes)

$$A_{m,n,j} = \frac{in}{m + \kappa^{1/2}\sigma_{m,n,j}} \cdot \frac{1}{E^{1/2}_{m,n,j}}$$

$$B_{m,n,j} = \frac{i}{2(m - \kappa^{1/2}\sigma_{m,n,j})} \cdot \frac{1}{E^{1/2}_{m,n,j}}$$

$$C_{m,n,j} = \frac{1}{E^{1/2}_{m,n,j}}$$

$E_{m,n,j}$ = the kinetic energy of one single mode integrated over the whole domain

$\sigma_{m,n,j}$ = the frequencies of the modes

The different $\sigma_{m,n,j}$'s satisfy the following dispersion relation:

$$\sigma^3_{m,n} - \sigma_{m,n}(m^2\kappa^{-1} + (2n+1)\kappa^{-1/2}) - m\kappa^{-1} = 0. \tag{2.6}$$

For some special choices of m and n the system (2.1)–(2.3) has solutions which are not automatically incorporated in (2.5). These are the Kelvin modes, the mixed Rossby-gravity modes (n

$= 0$; $m > 0$) and the sloshing modes ($m = 0$). The latter modes are sloshing across the equator with typical gravity frequencies. A feature of the sloshing mode, which is worthwhile pointing out can be seen from eq. (2.5). Since $A_{m,n,j}$ and $B_{m,n,j}$ both are purely imaginary, $C_{m,n,j}$ is real, and furthermore $m = 0$ (i.e. $e^{im\lambda} = 1$), a real value of the complex sloshing mode amplitude, means that we have no height field and only a v-component of the wind. If on the other hand the amplitude is imaginary, we have only a height field and a u-component of the wind.

We can now construct a low-order system by selecting a number of modes which interact non-linearly with each other. In the present study, we want to use a system small enough to be treated analytically (at least partly) but still large enough to contain non-trivial non-linear interactions. Furthermore, we require that the Machenhauer initialization procedure generates non-trivial gravity fields. A low-order system that fulfils these requirements is one containing one Rossby mode and two gravity modes selected in the following way. The Rossby mode is symmetric around the equator and has a zonal wavenumber k (i.e., $m = k$, $n = 1$, $j = 1$); one gravity mode which is a symmetric sloshing mode (i.e., $m = 0$, $n = 1, j = 2$); the third mode is a symmetric eastward propagating gravity mode with zonal wavenumber $2k$ (i.e., $m = 2k$, $n = 1, j = 2$).

A low-order model like this only crudely describes the motions in the real atmosphere, but it still contains some of the most important features of a primitive weather prediction model, namely:

(a) the Rossby mode which has a frequency and a balance between the wind and height fields that resembles the real atmosphere;
(b) gravity modes which can describe high-frequency oscillations.

There are of course, other possible three-mode systems, but this is the only type that combines the following features which we believe are essential.

(1) Both gravity modes are forced by wave–wave interaction of Rossby–Rossby type.
(2) All three modes contain non-linear interactions with both the others.

Let us introduce the following notation:

$D_S = X_r + iX_i$
$D_R = Y_r + iY_i$
$D_G = Z_r + iZ_i$

where S, R and G stand for sloshing, Rossby and gravity respectively.

We can now write the adiabatic low-order model as a system of six real ordinary differential equations:

$$\frac{d}{dt} x_r = \sigma_S x_i - \alpha_2(y_r^2 + y_i^2) - \alpha_3(z_r^2 + z_i^2), \tag{2.7}$$

$$\frac{d}{dt} x_i = -\sigma_S x_r - \alpha_1 x_r x_i, \tag{2.8}$$

$$\frac{d}{dt} y_r = \sigma_R y_i - \beta_1 x_r y_r + \beta_2 x_i y_i - \beta_3(y_r z_r + y_i z_i), \tag{2.9}$$

$$\frac{d}{dt} y_i = -\sigma_R y_r - \beta_1 x_r y_i - \beta_2 x_i y_r - \beta_3(y_r z_i - y_i z_r), \tag{2.10}$$

$$\frac{d}{dt} z_r = \sigma_G z_i - \gamma_1 x_r z_r - \gamma_2(y_r^2 - y_i^2) + \gamma_3 x_i z_i, \tag{2.11}$$

$$\frac{d}{dt} z_i = -\sigma_G z_r - \gamma_1 x_r z_i - 2\gamma_2 y_r y_i - \gamma_3 x_i z_r. \tag{2.12}$$

In these equations the α's, β's and γ's are the interaction coefficients describing the non-linear wave-to-wave interaction. Table 1 shows the interaction coefficients for $k = 6$. $\kappa = 10$ and $\varepsilon = 0.05$.

In some experiments we have included a simple non-adiabatic forcing in the model according to:

$$\frac{\partial u}{\partial t} - \theta v + \frac{\partial \phi}{\partial \lambda} + \varepsilon\left(u\frac{\partial u}{\partial \lambda} + v\frac{\partial u}{\partial \theta}\right) = F_u, \tag{2.13}$$

$$\frac{\partial v}{\partial t} + \theta u + \frac{\partial \phi}{\partial \theta} + \varepsilon\left(u\frac{\partial v}{\partial \lambda} + v\frac{\partial v}{\partial \theta}\right) = F_v, \tag{2.14}$$

$$\frac{\partial \phi}{\partial t} + \kappa^{-1}\left(\frac{\partial u}{\partial \lambda} + \frac{\partial v}{\partial \theta}\right) + \varepsilon\left(\frac{\partial u\phi}{\partial \lambda} + \frac{\partial v\phi}{\partial \theta}\right) = F_\phi + \varepsilon\left(\frac{\partial u\phi_b}{\partial \lambda} + \frac{\partial v\phi_b}{\partial \theta}\right). \tag{2.15}$$

F_u, F_v and F_ϕ represent a spatially-fixed forcing which does not interact non-linearly with the dynamical fields (e.g., differential heating from land and sea distribution). It may also be thought of as

Table 1. *The interaction coefficients and the eigenfrequencies (σ) for $\kappa = 10$ ($H \approx 8792.8$ m). $\varepsilon = 0.05$ ($U \approx 50$ m s^{-1}) and $k = 6$*

i	α_i	β_i	γ_i	σ
1	$1.43 \cdot 10^{-3}$	$-2.77 \cdot 10^{-4}$	$-9.64 \cdot 10^{-4}$	$\sigma_S = 0.97$
2	$1.20 \cdot 10^{-2}$	$-4.33 \cdot 10^{-2}$	$-2.03 \cdot 10^{-3}$	$\sigma_R = -0.13$
3	$4.69 \cdot 10^{-4}$	$9.58 \cdot 10^{-3}$	$-1.27 \cdot 10^{-1}$	$\sigma_G = 3.96$

the coupling between different vertical modes appearing in multilevel models. The terms including ϕ_b describe non-linear orographic interactions in the model.

In order to include the physical forcing into eqs. (2.7)–(2.12), we have to expand the fields according to:

$$F_u = \sum_{m=-M}^{M} \sum_{n=0}^{N} (f_{u_r}^{m,n} + i f_{u_i}^{m,n}) H_n(\eta)\, e^{-\eta^2/2 + im\lambda}, \tag{2.16}$$

$$F_v = \sum_{m=-M}^{M} \sum_{n=0}^{N} (f_{v_r}^{m,n} + i f_{v_i}^{m,n}) H_n(\eta)\, e^{-\eta^2/2 + im\lambda}, \tag{2.17}$$

$$F_\phi = \sum_{m=-M}^{M} \sum_{n=0}^{N} (f_{\phi_r}^{m,n} + i f_{\phi_i}^{m,n}) H_n(\eta)\, e^{-\eta^2/2 + im\lambda}, \tag{2.18}$$

$$\phi_b = \sum_{n_2=0}^{I} (\phi_{b_r}^{k,2n_2} + i\phi_{b_i}^{k,2n_2}) H_{2n_2}(\eta)\, e^{-\eta^2/2 + ik\lambda}. \tag{2.19}$$

For simplicity, the mountains are symmetric around the equator ($n = 0$ and $n = 2$ is used) and have components only in the wave number of the Rossby mode (i.e., $m = k$).

If we introduce expansions (2.16)–(2.19) into system (2.13)–(2.15), expand the dynamical fields in their normal modes and make use of the orthogonality properties of the normal modes we will find that when forcing is included, the system (2.7)–(2.12) is replaced by:

$$\frac{d}{dt} x_r = \sigma_S x_i - \alpha_2(y_r^2 + y_i^2) - \alpha_3(z_r^2 + z_i^2) + F_{Srf}, \tag{2.20}$$

$$\frac{d}{dt} x_i = -\sigma_S x_r - \alpha_1 x_r x_i + F_{Sib} + F_{Sif}, \tag{2.21}$$

$$\frac{d}{dt} y_r = \sigma_R y_i - \beta_1 x_r y_r + \beta_2 x_i y_i - \beta_3(y_r z_r + y_i z_i) + F_{Rrb} + F_{Rrf}, \tag{2.22}$$

$$\frac{d}{dt} y_i = -\sigma_R y_R - \beta_1 x_r y_i - \beta_2 x_i y_r - \beta_3(y_r z_i - y_i z_r) + F_{Rib} + F_{Rif}, \tag{2.23}$$

$$\frac{d}{dt} z_r = \sigma_G z_i - \gamma_1 x_r z_r - \gamma_2(y_r^2 - y_i^2) + \gamma_3 x_i z_i + F_{Grb} + F_{Grf}, \tag{2.24}$$

$$\frac{d}{dt} z_i = -\sigma_G z_r - \gamma_1 x_r z_i - 2\gamma_2 y_r y_i - \gamma_3 x_i z_r + F_{Gib} + F_{Gif}, \tag{2.25}$$

where F_{Sib}, F_{Rrb}, ... contain the interactions with mountains and F_{Srf}, F_{Sif}, F_{Rrf}, ... describe the spatially-fixed forcing.

If we denote the interaction coefficients describing the physical forcing with δ we can write the F's in the following way (let us choose F_{Srf}, F_{Grb} and F_{Grf} as examples):

$$F_{Srf} = \delta_{S1} f_{v_r}^{0,1}, \tag{2.26}$$

$$F_{Grb} = \delta_{G1}(y_r \phi_{b_i}^{k,0} + y_i \phi_{b_r}^{k,0}) + \delta_{G2}(y_r \phi_{b_i}^{k,2} + y_i \phi_{b_r}^{k,2}), \tag{2.27}$$

$$F_{Grf} = \delta_{G3} f_{u_i}^{2k,0} + \delta_{G4} f_{u_i}^{2k,2} + \delta_{G5} f_{v_r}^{2k,1} + \delta_{G6} f_{\phi_i}^{2k,0} + \delta_{G7} f_{\phi_i}^{2k,2}. \tag{2.28}$$

3. The no-forcing case

In the case of no-forcing, the system (2.7)–(2.12) defines the model. The Machenhauer initialization method determines, for given Rossby amplitudes, the gravity amplitudes in such a way that the tendencies in the gravity amplitudes are zero initially. This means in our model that we shall require;

$$\frac{dx_r}{dt} = \frac{dx_i}{dt} = \frac{dz_r}{dt} = \frac{dz_i}{dt} = 0. \tag{3.1}$$

Conditions (3.1) give us the following system of non-linear equations:

$$\sigma_S x_i - \alpha_2(y_r^2 + y_i^2) - \alpha_3(z_r^2 + z_i^2) = 0, \tag{3.2}$$

$$-\sigma_S x_r - \alpha_1 x_r x_l = 0, \tag{3.3}$$

$$\sigma_G z_l - \gamma_1 x_r z_r - \gamma_2(y_r^2 - y_l^2) + \gamma_3 x_l z_l = 0, \tag{3.4}$$

$$-\sigma_G z_r - \gamma_1 x_r z_l - 2\gamma_2 y_r y_l - \gamma_3 x_l z_r = 0 \tag{3.5}$$

Let us choose a coordinate system such that the Rossby amplitude is a real quantity (i.e., $y_r \neq 0$; $y_l = 0$). This means that eqs. (3.3) and (3.5) are independent of the Rossby amplitude:

$$-\sigma_S x_r - \alpha_1 x_r x_l = 0, \tag{3.6}$$

$$-\sigma_G z_r - \gamma_1 x_r z_l - \gamma_3 x_l z_r = 0. \tag{3.7}$$

These equations can be satisfied only if

(I) $x_r = z_r = 0$, (x_l, z_l arbitrary),

or (II) $x_r = 0; x_l = -\dfrac{\sigma_G}{\gamma_3}$ (z_l, z_r arbitrary),

or (III) $x_l = -\dfrac{\sigma_S}{\alpha_1}; \quad z_r = \dfrac{-\gamma_1 x_r z_l}{\sigma_G - \gamma_3 \sigma_S/\alpha_1}$ (x_r, z_l arbitrary).

If alternative (I) is true, then eqs. (3.2) and (3.4) yield:

$$\sigma_S x_l - \alpha_2 y_r^2 - \alpha_3 z_l^2 = 0, \tag{3.8}$$

$$\sigma_G z_l - \gamma_2 y_r^2 + \gamma_3 x_l z_l = 0. \tag{3.9}$$

Alternative (II) leads to:

$$-\frac{\sigma_S \sigma_G}{\gamma_3} - \alpha_2 y_r^2 - \alpha_3(z_r^2 + z_l^2) = 0 \tag{3.10}$$

$$\sigma_G z_l - \gamma_2 y_r^2 - \sigma_G z_l = 0. \tag{3.11}$$

$$\Rightarrow y_r^2 = 0,$$

i.e. alternative (II) is of no interest to us.

The third alternative is more complicated, but by introducing

$$\gamma_4 = \frac{\gamma_1}{\sigma_G - \gamma_3 \sigma_S/\alpha_1},$$

we can rewrite eq. (3.2) according to

$$-\frac{\sigma_S^2}{\alpha_1} - \alpha_2 y_r^2 - \alpha_3 z_l^2(\gamma_4^2 x_r^2 + 1) = 0$$

$$\Rightarrow z_l^2 = -\left(\frac{\sigma_S^2}{\alpha_1} + \alpha_2 y_r^2\right) \Big/ (\gamma_4^2 x_r^2 + 1)\alpha_3. \tag{3.12}$$

Eq. (3.12) cannot be satisfied for arbitrary values of α_1, α_2 and α_3, since the condition

$$z_l^2 \geqslant 0$$

must also be satisfied.

Since, in this investigation, α_1, α_2 and α_3 are all positive, (3.12) cannot be satisfied and therefore we have to reject alternative (III).

We can also find another reason to exclude alternatives (II) and (III) by considering the iterative method used to solve the non-linear system (3.2)–(3.5). We can write iteration number $\nu + 1$ as:

$$x_l^{(\nu+1)} = (\alpha_2 y_r^2 + \alpha_3[(z_r^{(\nu)})^2 + (z_l^{(\nu)})^2])/\sigma_S, \tag{3.13}$$

$$x_r^{(\nu+1)} = -\alpha_1 x_r^{(\nu)} x_l^{(\nu)}/\sigma_S, \tag{3.14}$$

$$z_l^{(\nu+1)} = (\gamma_1 x_r^{(\nu)} z_r^{(\nu)} + \gamma_2 y_r^2 - \gamma_3 x_l^{(\nu)} z_l^{(\nu)})/\sigma_G, \tag{3.15}$$

$$z_r^{(\nu+1)} = (-\gamma_1 x_r^{(\nu)} z_l^{(\nu)} - \gamma_3 x_l^{(\nu)} z_r^{(\nu)})/\sigma_G. \tag{3.16}$$

If we now start the iterative procedure with all gravity amplitudes zero (i.e., $x_r^{(0)} = x_l^{(0)} = z_r^{(0)} = z_l^{(0)} = 0$), then we can see from eqs. (3.14) and (3.16) that $x_r^{(\nu)}$ and $z_r^{(\nu)}$ will remain zero for all values of ν, that is, the iterative procedure leads to the solution given by alternative (I).

In order to simplify the investigation of alternative (I) let us rewrite eqs. (3.8) and (3.9):

$$x_l = \frac{\alpha_3}{\sigma_S} z_l^2 + \frac{\alpha_2}{\sigma_S} y_r^2, \tag{3.17}$$

$$x_l = \frac{\gamma_2}{\gamma_3} y_r^2 \frac{1}{z_l} - \frac{\sigma_G}{\gamma_3}. \tag{3.18}$$

Eq. (3.17) represents a parabola and eq. (3.18) a hyperbola. These two curves are plotted in Fig. 1 in a qualitative way, in the sense that the signs, but not necessarily the magnitudes, of the interaction coefficients and the frequencies are correct. We can see from Fig. 1, that generally there are more than one possible initial state, that satisfy the Machenhauer condition.

In Table 2 the values of the gravity amplitudes satisfying the Machenhauer condition are tabulated for different values of the depth and for $k = 6$, $y_r = 1$, $\varepsilon = 0.05$.

Table 3 contains the ratios between the terms describing the Rossby–Rossby interaction and the

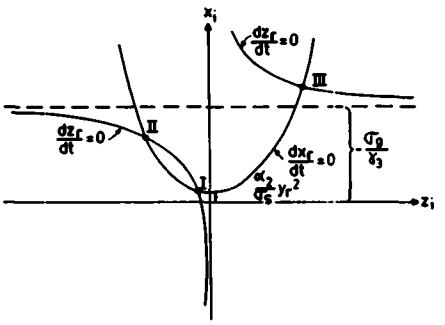

Fig. 1. The Machenhauer condition. The parabola illustrates $dx_r/dt = 0$ and the hyperbola $dz_r/dt = 0$. The intersections represent states that satisfy the Machenhauer condition.

Table 3. *Intercomparison of the terms in the equations defining the initial state according to Machenhauer's method.*

Solution	$\left\|\frac{\alpha_2 y_r^2}{\alpha_3 z_l^2}\right\|$	$\left\|\frac{\gamma_2 y_r^2}{\gamma_3 x_l z_l}\right\|$	
(I)	$9.8 \cdot 10^7$	$2.7 \cdot 10^3$	$\kappa = 10$
(II)	$4.1 \cdot 10^{-4}$	$2.1 \cdot 10^{-6}$	($H = 8792.6$ m)
(III)	$4.1 \cdot 10^{-4}$	$2.1 \cdot 10^{-6}$	
(I)	$3.7 \cdot 10^1$	$1.3 \cdot 10^1$	$\kappa = 10^5$
(II)	$1.9 \cdot 10^{-1}$	$7.3 \cdot 10^{-2}$	($H = 0.9$ m)
(III)	$1.5 \cdot 10^{-1}$	$6.1 \cdot 10^{-2}$	

Solution (I) corresponds to the solution with relatively small gravity amplitudes. Solutions (II) and (III) correspond to the solutions with relatively large gravity amplitudes. $k = 6$; $\varepsilon = 0.05$ and $y_r = 1$.

gravity–gravity interaction in the two gravity equations (cf eqs. (3.8) and 3.9)) for two values of the depth.

Tables 2 and 3 and the fact that in a multilevel model, $y_r = 1$ is too large, except for the external mode, help us classify the three solutions into two groups:

(1) containing solution I, in which:
   (a) the gravity amplitudes < the Rossby amplitude;
   (b) a balance exists between the linear gravity term and the term describing the Rossby–Rossby interaction.

(2) containing solutions II and III, in which:
   (a) the gravity amplitudes > the Rossby amplitude;
   (b) a balance exists between the linear gravity term and the term describing the gravity–gravity interaction.

In this paper we will henceforth refer to the solutions in group (1) as the "true Machenhauer solutions".

Now let us investigate to which point in phase space the iterative Machenhauer procedure converges. We again choose $y_l = 0$ $x_r = z_r = 0$. Eqs. (3.13) and (3.15) then define the iterative procedure:

$$x_l^{(\nu+1)} = \frac{\alpha_2 y_r^2}{\sigma_S} + \frac{\alpha_3 (z^{(\nu)})^2}{\sigma_S}, \tag{3.19}$$

$$z_l^{(\nu+1)} = \frac{\gamma_2 y_r^2}{\sigma_G} - \frac{\gamma_3 x_l^{(\nu)} z_l^{(\nu)}}{\sigma_G}. \tag{3.20}$$

Introduce

$$x_l = \tilde{x}_l + x_l', \qquad z_l = \tilde{z}_l + z_l',$$

where $\tilde{x}_l$ and $\tilde{z}_l$ satisfy the initial condition, and

Table 2. *Gravity amplitudes satisfying the Machenhauer condition; $\varepsilon = 0.05$, $k = 6$, $y_r = 1$*

Solution	I		II		III	
$H(m)$	x_l	z_l	x_l	z_l	x_l	z_l
8792.8	$1.2 \cdot 10^{-2}$	$-5.1 \cdot 10^{-4}$	$3.1 \cdot 10^1$	$-2.5 \cdot 10^2$	$3.1 \cdot 10^1$	$2.5 \cdot 10^2$
879.3	$3.4 \cdot 10^{-2}$	$-3.2 \cdot 10^{-3}$	$1.1 \cdot 10^1$	$-5.6 \cdot 10^1$	$1.1 \cdot 10^1$	$5.6 \cdot 10^1$
87.9	$7.3 \cdot 10^{-2}$	$-1.6 \cdot 10^{-2}$	$4.8 \cdot 10^0$	$-1.6 \cdot 10^1$	$4.8 \cdot 10^0$	$1.6 \cdot 10^1$
8.8	$1.1 \cdot 10^{-1}$	$-6.8 \cdot 10^{-2}$	$2.5 \cdot 10^0$	$-5.8 \cdot 10^0$	$2.6 \cdot 10^0$	$5.9 \cdot 10^0$
0.9	$1.3 \cdot 10^{-1}$	$-2.2 \cdot 10^{-1}$	$1.8 \cdot 10^0$	$-2.9 \cdot 10^0$	$2.0 \cdot 10^0$	$3.1 \cdot 10^0$

$$\frac{\alpha_2 y_r^2}{\sigma_S} = a_1, \frac{\alpha_3}{\sigma_S} = a_2, \frac{\gamma_2 y_r^2}{\sigma_G} = b_1, -\frac{\gamma_3}{\sigma_G} = b_2.$$

The equations may then be written:

$$x_l^{(\nu+1)'} = 2a_2 \tilde{z}_l z^{(\nu)'} + a_2 (z^{(\nu)'})^2, \tag{3.21}$$

$$z_l^{(\nu+1)'} = b_2 (\tilde{x} z^{(\nu)'} + x^{(\nu)'} \tilde{z} + x^{(\nu)'} z^{(\nu)'}). \tag{3.22}$$

A linearization of this system yields:

$$\begin{pmatrix} x^{(\nu+1)'} \\ z^{(\nu+1)'} \end{pmatrix} = \begin{pmatrix} 0 & 2a_2\tilde{z} \\ b_2\tilde{z} & b_2\tilde{x} \end{pmatrix} \begin{pmatrix} x^{(\nu)'} \\ z^{(\nu)'} \end{pmatrix}. \tag{3.23}$$

The initialization procedure will converge only if the eigenvalues of system (3.23) fulfil the condition

$$|\lambda| < 1.$$

The eigenvalues are the solutions to:

$$-\lambda(-\lambda + b_2\tilde{x}) - 2a_2 b_2 \tilde{z}^2 = 0, \tag{3.24}$$

and the condition $\lambda > -1$ yields that the solution $(\tilde{x}_l, \tilde{z}_l)$ must be situated inside (on the concave side of) the parabola:

$$x_l = -\frac{1}{b_2} + 2a_2 z_l^2, \tag{3.25}$$

while the condition $\lambda < 1$ yields that the solution must be inside the parabola

$$x_l = \frac{1}{b_2} - 2a_2 z_l^2. \tag{3.26}$$

We shall deduce some further properties by making use of the two equations defining $dx_r/dt = 0$ (eq. (3.17)) and $dz_r/dt = 0$ (eq. (3.18)) which we can rewrite as:

$$x_l = a_1 + a_2 z_l^2, \tag{3.27}$$

$$x_l = -\frac{b_1}{b_2}\frac{1}{z_l} + \frac{1}{b_2}. \tag{3.28}$$

First we note that the parabola (3.26) and the horizontal asymptote to the hyperbola (3.28) ($x_l = 1/b_2$) intersect at $z_l = 0$. Secondly, if we differentiate eqs. (3.27) and (3.28) with respect to z_l,

$$\frac{d}{dz_l}_{\text{parabola}} x_l = 2a_2 z_l, \tag{3.29}$$

$$\frac{d}{dz_l}_{\text{hyperbola}} x_l = \frac{b_1}{b_2}\frac{1}{z_l^2}, \tag{3.30}$$

we find that the parabola defining $dx_r/dt = 0$ has the same slope as the hyperbola defining $dz_r/dt = 0$ when

$$2a_2 z_l = \frac{b_1}{b_2}\frac{1}{z_l^2}. \tag{3.31}$$

We find the intersection between the parabola limiting the region in which $\lambda < 1$ (eq. (3.26)) and the hyperbola (3.28) from

$$\frac{1}{b_2} - 2a_2 z_l^2 = -\frac{b_1}{b_2}\frac{1}{z_l} + \frac{1}{b_2}$$

$$\Rightarrow 2a_2 z_l = \frac{b_1}{b_2}\frac{1}{z_l^2}.$$

This equation is the same as (3.31), which means that the parabola (3.26) intersects the hyperbola (3.28) at the value of z_l where the hyperbola has the same slope as the parabola (3.27). For obvious reasons (cf. Fig. 1), this value of z_l has to be situated somewhere between the z_l's defining solution (I) and solution (II) in Fig. 1. This means that if there are three solutions that satisfy the Machenhauer condition, the iterative procedure can converge only to the "true Machenhauer solution" as illustrated in Fig. 2. If the parameters are such that we only have one solution (e.g., if the parabola $dx_r/dt = 0$ is shifted high enough so that solutions (I) and (II) disappear), the remaining solution is always above the asymptote and the iterative procedure cannot find it.

The next step in order to understand the mathematical properties of the system will be to

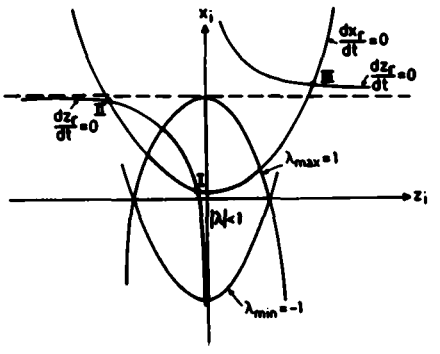

Fig. 2. The convergence of the iterative Machenhauer procedure. The procedure diverges outside the hatched region.

investigate what happens when we vary the magnitude of the meteorological amplitude, y_r. From eq. (3.17), we see that if we increase y_r, the parabola will be lifted (cf. Fig. 1). In the same way, eq. (3.18) tells us that an increase of y_r would move the branches of the hyperbola somewhat away from their asymptote. These features are illustrated in Fig. 3. In this figure, we see that when y_r is increased, the solutions (I) and (II) will become closer, and obviously there must be a critical value of y_r where we lose the two solutions (I) and (II).

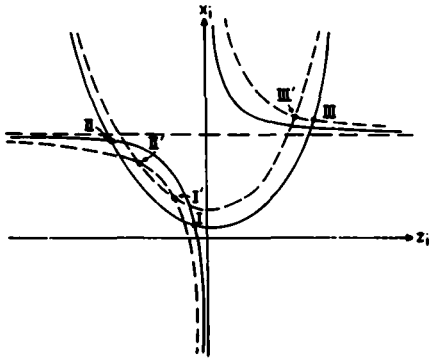

Fig. 3. The influence of changing the Rossby amplitude y_r. Full line is for $y_r = y_{r1}$, dashed line for $y_r > y_{r1}$.

We can also describe the same feature by eliminating x_t from eqs. (3.17) and (3.18):

$$\Rightarrow y_r^2 = \frac{z_t\left(\frac{\sigma_G}{\gamma_3} + \frac{\alpha_3}{\sigma_S} z_t^2\right)}{\frac{\gamma_2}{\gamma_3} - \frac{\alpha_2}{\sigma_S} z_t}. \tag{3.32}$$

Fig. 4 shows characteristics of eq. (3.32) with the current signs of the interaction coefficients. We see that for small values of y_r^2, there are three possible values of z_t, that is, three solutions, and that when $y_r^2 > y_{r\text{crit}}^2$ the two solutions where $z_t < 0$ are lost.

In Fig. 5, eq. (3.32) is illustrated for different values of κ that is, for different values of the depth of the fluid. Fig. 5 tells us that if we decrease the depth of the fluid (increase κ), the critical value of y_r^2 will also decrease.

Fig. 6 shows the values of $y_{r\text{crit}}^2$ for $k = 6$.

4. The case with forcing

When we include physical forcing in the model, the appropriate equations are given by eqs. (2.20)–(2.25). The Machenhauer condition then leads to (still for the case $y_t = 0$):

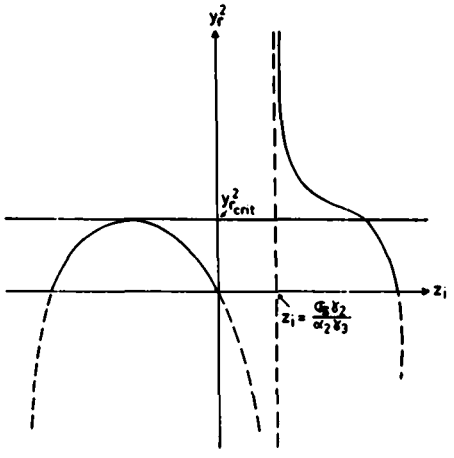

Fig. 4. The values of one gravity amplitude (z_t) satisfying the Machenhauer condition for different values of the Rossby amplitude (y_r).

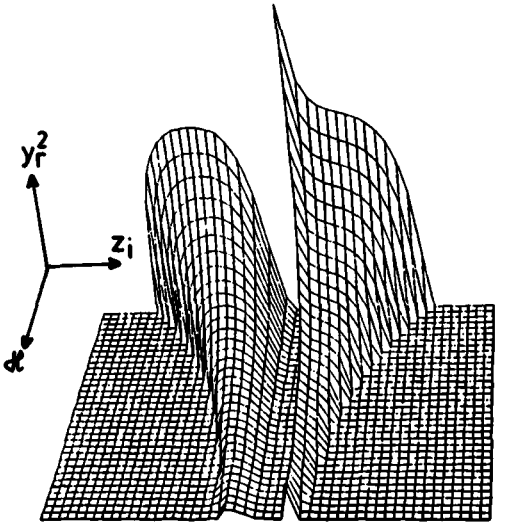

Fig. 5. Same as Fig. 4 but the variation of the equivalent depth (H) is included. $\kappa \sim 1/H$.

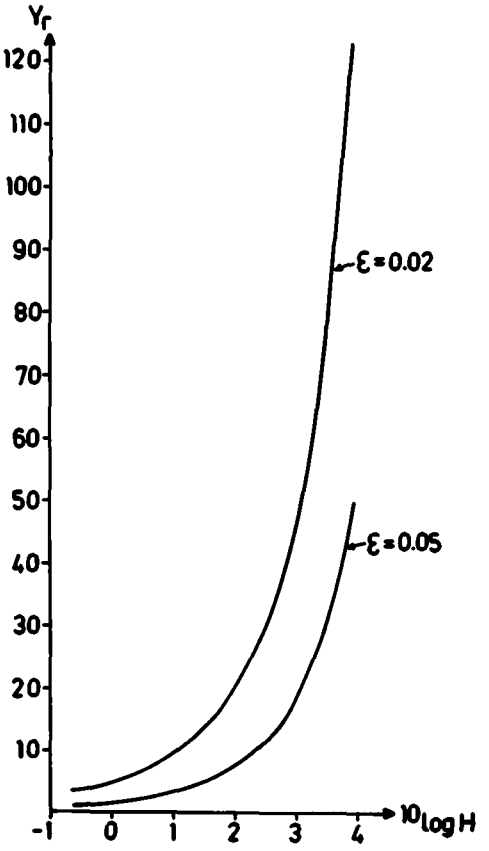

Fig. 6. Critical values of the Rossby amplitude ($y_{r\,crit}$) beyond which "the true Machenhauer solution" does not exist. $k = 6$.

$$\sigma_S x_l - \alpha_2 y_r^2 - \alpha_3(z_r^2 + z_l^2) + F_{Srf} = 0, \tag{4.1}$$

$$-\sigma_S x_r - \alpha_1 x_r x_l + F_{Slb} + F_{Slf} = 0, \tag{4.2}$$

$$\sigma_G z_l - \gamma_1 x_r z_r - \gamma_2 y_r^2 + \gamma_3 x_l z_l + F_{Grb} + F_{Grf} = 0, \tag{4.3}$$

$$-\sigma_G z_r - \gamma_1 x_r z_l - \gamma_3 x_l z_r + F_{Glb} + F_{Glf} = 0. \tag{4.4}$$

Let us investigate whether the mountains or the spatially-fixed forcing can cause the Machenhauer procedure to diverge. If, in order to simplify the investigation, we assume that the forcing does not contribute to the imaginary part of the gravity amplitudes, and furthermore that $y_l = 0$, the system defining the initial state can be written (cf. eqs. (2.20)–(2.25)):

$$\sigma_S x_l - \alpha_2 y_r^2 - \alpha_3(z_r^2 + z_l^2) + F_{Srf} = 0, \tag{4.5}$$

$$-\sigma_S x_r - \alpha_1 x_r x_l = 0, \tag{4.6}$$

$$\sigma_G z_l - \gamma_1 x_r z_r - \gamma_2 y_r^2 + \gamma_3 x_l z_l + F_{Grb} + F_{Grf} = 0, \tag{4.7}$$

$$-\sigma_G z_r - \gamma_1 x_r z_l - \gamma_3 x_l z_r = 0. \tag{4.8}$$

As in the case without forcing, we see that $x_r = z_r = 0$ satisfies eqs. (4.6 and 4.7) and also that these values of x_r and z_r are the same as those yielded by the iterative procedure. Therefore we again have to deal with a two-dimensional problem namely:

$$\sigma_S x_l - \alpha_2 y_r^2 - \alpha_3 z_l^2 + F_{Srf} = 0, \tag{4.9}$$

$$\sigma_G z_l - \gamma_2 y_r^2 + \gamma_3 x_l z_l + F_{Grb} + F_{Grf} = 0. \tag{4.10}$$

We found earlier that the Machenhauer procedure diverges in the case without forcing if $y_r^2 > y_{r\,crit}^2$. By setting

$$F_{Srf} = -\alpha_2 y_{r\,crit}^2, \tag{4.11}$$

$$F_{Grb} + F_{Grf} = -\gamma_2 y_{r\,crit}^2, \tag{4.12}$$

we can estimate the forcing necessary to violate the non-linear normal-mode initialization. From eqs. (2.26)–(2.28) we get:

$$F_{Srf} = \delta_{S1} f_{v_r}^{0,1}, \tag{4.13}$$

$$F_{Grb} = \delta_{G1}(y_r \phi_{b_l}^{k,0} + y_l \phi_{b_r}^{k,0}) + \delta_{G2}(y_r \phi_{b_l}^{k,2} + y_l \phi_{b_r}^{k,0}), \tag{4.14}$$

$$F_{Grf} = \delta_{G3} f_{u_l}^{2k,0} + \delta_{G4} f_{u_l}^{2k,2} + \delta_{G5} f_{v_r}^{2k,1} + \delta_{G6} f_{\phi_l}^{2k,0} + \delta_{G7} f_{\phi_l}^{2k,2}. \tag{4.15}$$

The forcing on the v-component of the wind in wavenumber zero calculated from eqs. (4.13) and (4.11) ($k = 6$, $\varepsilon = 0.05$) is tabulated in Table 4. We

Table 4. *Critical values of the spatially fixed forcing on the v-momentum* ($k = 6$; $\varepsilon = 0.05$)

H(m)	$f_{v_r}^{0,1} = -\frac{\alpha_2}{\delta_{S1}} y_{r\,crit}^2$	Acceleration (m s^{-1} h^{-1}) at 30° lat
8792.8	−5.6	−147
879.3	−0.94	−25.67
87.9	−0.21	−5.49
8.8	−0.04	−1.1
0.9	−0.008	−0.2

Table 5. *Critical values of the orographic forcing ($k = 6$; $\varepsilon = 0.05$)*

H (m)	$\phi_{bl}^{k,0} = -\frac{\gamma_2}{\delta_{G1}} y_{rcrit}$	Height of the mountains (m) at the equator	$\phi_{bl}^{k,2} = \frac{\gamma_2}{\delta_{G2}} y_{rcrit}$	Height (m) latitude $\approx 50°$
8792.6	4.93	23,353	24.89	117,936
879.3	0.19	883	−0.30	2,812
87.9	0.012	60	−0.009	86
8.8	0.0012	6	−0.0007	7
0.9	0.0001	0.7	−0.00003	0.3

Table 6. *Critical values of the spatially fixed forcing on the u-momentum ($k = 6$; $\varepsilon = 0.05$)*

H (m)	$f_{ul}^{2k,2} = -\frac{\gamma_2}{\delta_{G4}} y_{rcrit}^2$	Acceleration (m s^{-1} h^{-1}) at 45° lat
8792.8	0.58	31
879.3	0.13	7
87.9	0.05	2
8.8	0.010	0.5
0.9	0.011	0.6

Table 7. *Critical values of the spatially fixed forcing on the height-field ($k = 6$; $\varepsilon = 0.05$)*

H (m)	$f_{\phi_l}^{2k,2} = -\frac{\gamma_2}{\delta_{G7}} y_{rcrit}^2$	Divergence (s^{-1}) at 45° lat
8792.8	0.18	$2.7 \cdot 10^{-5}$
879.3	0.01	$1.9 \cdot 10^{-6}$
87.9	0.001	$2.1 \cdot 10^{-7}$
8.8	0.0001	$1.5 \cdot 10^{-8}$
0.9	0.00004	$5.1 \cdot 10^{-9}$

see that for large values of the equivalent depth, a very strong forcing is needed in order to reach the region where "the true Machenhauer solution" disappears. For small values of the equivalent depth, however, a very moderate forcing is sufficient to risk the initialization procedure. The negative sign of the accelerations in Table 4 means that the acceleration is directed towards the equator. Table 5 shows the effect of mountains for wavenumber $m = k = 6$ calculated from eqs. (4.14) and (4.12). Table 6 displays the forcing on the u-component of the wind in wavenumber $2k = 12$ and $n = 2$, and Table 7 the forcing on the height field in wavenumber $2k = 12$, $n = 2$. All these tables demonstrate the same trend; when the depth of the fluid is large, very strong forcing is required in order to lose the "the true Machenhauer solution". For the depth corresponding to the external mode, the forcing required is unlikely to occur, but if we diminish the depth to $\frac{1}{10}$ of the external one, the forcing is quite conceivable. For the smallest values of the depth, the forcing needed is slight.

5. Summary and conclusions

In this investigation, we have tried to gain insight into the non-linear normal mode initialization by using a low-order shallow water model at the equator. We have put special emphasis on trying to find possible explanations for the fact that the iterative non-linear normal-mode procedure tends to diverge, when the equivalent depth is diminished or when forcing is included in the procedure. The model contains only three modes; one Rossby mode, one gravity-inertia mode and one sloshing mode. All three modes are symmetric with respect to the equator. We have also included forcing in the model in the form of momentum and height forcing fixed in space and also orography. The orography has the same wavenumber as the Rossby mode.

We defined the initial state by requiring the tendencies of the gravity-inertia mode and of the sloshing mode to be equal to zero. We were able to reduce the resulting system to one containing only two variables. From this two-dimensional system we deduced that generally there are three different states that satisfy the initial conditions. Except for very small depth of the fluid, it is obvious that two of these possible initial states have unrealistically large gravity amplitudes. Furthermore, the states with relatively large gravity amplitudes are charac-

terized by an approximative balance between the linear term in the gravity equation and the non-linear term describing the interaction between the gravity modes. This means that these initial states are essentially independent of the Rossby motion. From a meteorological point of view, such initial states can hardly be accepted, since the idea with the initialization is to adjust the motion that is defined by the Rossby modes, in order to avoid high-frequency oscillation. An investigation of the iterative procedure normally used to solve the non-linear system, showed that this procedure converges only to the initial state that has the smallest gravity and amplitudes.

When we increased the Rossby amplitude, which acts like a forcing to the system defined by the initial conditions, we found a critical value of the Rossby amplitude beyond which two of the possible initial states do not exist.

One of these is the realistic state, defined by small gravity amplitudes, to which the iterative procedure converges in the case of smaller Rossby amplitudes. The critical value of the Rossby amplitude also becomes smaller when the depth of the fluid is diminished. Since the Rossby amplitudes in a multilevel model also decrease with diminishing depth, we cannot say that these results imply that the reason for which the non-linear normal mode initialization procedure diverges for small values of the equivalent depth, is that a relevant solution does not exist, but the results point at this as a possible explanation.

In the case with spatially fixed forcing, we avoided the complexity of the four-dimensional problem by choosing the forcing in such a way that we could again eliminate two equations from the system defining the initial state. It was then clear that this type of forcing plays the same rôle in the initialization procedure, as does the forcing from the Rossby wave. By using the results from the case without forcing, we could then calculate the magnitude of the forcing necessary in order to lose the meteorologically relevant solution. These calculations showed that the critical forcing is very strong for large depths and that it decreases with decreasing fluid depth. For small values of the depth, the critical forcing becomes extremely small; for example, when $H = 0.9$ m, the height of the critical mountains is 0.1 m. Although the simple model of this investigation is far from the complex models used for weather prediction, these results make it likely that the non-linear normal mode initialization procedure diverges when forcing is included, because the relevant solution disappears.

A simplified model such as the one used in this investigation, does not contain all the complexity of a weather prediction model. For example, the truncation of the model does not allow for non-linear terms describing Rossby-gravity interaction in the gravity equations. An example of such an interaction is the advection by a mean wind, which might influence the convergence properties of the Machenhauer initialization (Phillips, 1981; Ballish, 1981). But, since the model is able to describe motion on two different time scales, as well as non-trivial non-linear interactions between these two types of motion, it still contains some of the most important features involved in the initialization process. The results from an investigation using such a simplified model can never tell the whole truth of the full problem, but they can give us clues of how to understand and how to attack the more complex problems in a weather prediction model.

The fact that, in our simplified model, there are sometimes no acceptable solutions satisfying the Machenhauer condition, implies that this initial constraint should perhaps be modified. Daley (1978) suggested a variational technique, which also allows for a change in the Rossby modes in order to satisfy some additional initial constraint. Another approach is to allow the initial tendencies of the gravity amplitudes to be non-zero. An approach of this type is also physically relevant when we think of the initialization problem in terms of the slow manifold (Leith 1980). From this point of view, initial gravity tendencies are necessary, in order to allow the model to stay on the slow manifold. Such a property is inherent in the Baer and Tribbia (1977) procedure, since this generates initial non-zero gravity tendencies. However, the application of this method to weather prediction models is very complicated. Therefore, it is of great interest to further explore approaches in which the initial gravity tendencies are non-zero.

6. Acknowledgements

The author wants to thank Dr. Hilding Sundqvist and Prof. Bert Bolin for many valuable discussions and suggestions.

REFERENCES

Baer, F. 1977. Adjustment of initial conditions required to suppress gravity oscillations in non-linear flows. *Contrib. Atmos. Phys. 50*, 350–366.

Baer, F. and Tribbia, J. 1977. On complete filtering of gravity modes through non-linear initialization. *Mon. Wea. Rev. 105*, 1536–1539.

Ballish, B. 1981. A simple test of the initialization of gravity modes. *Mon. Wea. Rev. 109*, 1318–1321.

Daley, R. 1978. Variational non-linear normal-mode initialization. *Tellus 30*, 201–218.

Gollvik, S. and Thaning, L. 1980. A spectral primitive shallow water model on an equatorial β-plane. Dept. of Meteorology, University of Stockholm, Report DM-33. (Available from Library, Dept of Meteorology, University of Stockholm, Arrhenius Laboratory, S-106 91 Stockholm, Sweden.)

Leith, C. E. 1980. Non-linear normal-mode initialization and quasi-geostrophic theory. *J. Atmos. Sci. 37*, 958–968.

Machenhauer, B. 1977. On the dynamics of gravity oscillations in a shallow water-model, with applications to normal-mode initialization. *Contrib. Atmos. Phys. 50*, 253–271.

Phillips, N. 1981. Treatment of normal and abnormal modes. *Mon. Wea. Rev. 109*, 1117–1119.

Temperton, C. and Williamson, D. L. 1979. Normal mode initialization for a multi-level grid-point model. European Centre for Medium Range Weather Forecasts, Tech. Rep. No. 11.

Tribbia, J. 1979. Non-linear initialization on an equatorial β-plane. *Mon. Wea. Roy. 107*, 704–712.

Tribbia, J. 1981. Non-linear normal-mode balancing and the ellipticity condition. *Mon. Wea. Rev. 109*, 1751–1761.